

Should we reinforce the grid? Cost and emission optimization of electric vehicle charging under different transformer limits[☆]



N.B.G. Brinkel^{a,*,1}, W.L. Schram^{a,1}, T.A. AlSkaif^{a,b}, I. Lampropoulos^a, W.G.J.H.M. van Sark^a

^a Copernicus Institute of Sustainable Development, Utrecht University, Princetonlaan 8A, 3584 CB Utrecht, the Netherlands

^b Information Technology Group (INF), Wageningen University and Research (WUR), 6706 KN Wageningen, the Netherlands

HIGHLIGHTS

- A system perspective on cost and emission tradeoff of electric vehicle (EV) charging.
- A multi-objective optimization method of EV smart charging and vehicle-to-grid (V2G).
- Costs and CO₂ emissions of EV smart charging and V2G can be reduced simultaneously.
- Smart charging can mitigate grid congestion problems in case of high EV penetration.
- Cost and emissions of grid reinforcement outweigh benefits of increased flexibility.

ARTICLE INFO

Keywords:

Electric vehicle smart charging
Multi-objective optimization
Vehicle-to-grid
Grid reinforcements
Battery degradation
Average & marginal emission profiles

ABSTRACT

With high electric vehicle (EV) adoption, optimization of the charging process of EVs is becoming increasingly important. Although the CO₂ emission impact of EVs is heavily dependent on the generation mix at the moment of charging, emission minimization of EV charging receives limited attention. Generally, studies neglect the fact that cost and emission savings potential for EV charging can be constrained by the capacity limits of the low-voltage (LV) grid. Grid reinforcements provide EVs more freedom in minimizing charging costs and/or emissions, but also result in additional costs and emissions due to reinforcement of the grid. The first aim of this study is to present the trade-off between cost and emission minimization of EV charging. Second, to compare the costs and emissions of grid reinforcements with the potential cost and emission benefits of EV charging with grid reinforcements. This study proposes a method for multi-objective optimization of EV charging costs and/or emissions at low computational costs by aggregating individual EV batteries characteristics in a single EV charging model, considering vehicle-to-grid (V2G), EV battery degradation and the transformer capacity. The proposed method is applied to a case study grid in Utrecht, the Netherlands, using highly-detailed EV charging transaction data as input. The results of the analysis indicate that even when considering the current transformer capacity, cost savings up to 32.4% compared to uncontrolled EV charging are possible when using V2G. Emission minimization can reduce emissions by 23.6% while simultaneously reducing EV charging costs by 13.2%. This study also shows that in most cases, the extra cost or emission benefits of EV charging under a higher transformer capacity limit do not outweigh the cost and emissions for upgrading that transformer.

1. Introduction

With the substantial increase in electric vehicle (EV) charging transactions in low-voltage (LV) grids, optimization of the EV charging

process receives growing attention. Currently, most EVs charge in an uncontrolled manner; the EV starts charging directly after connecting to the charging station, until its charging requirement is met. This charging strategy is generally regarded as undesirable, as a large share of

[☆] This study was supported by the European Regional Development Fund (ERDF) 'EFRO Kansen voor West II' in the project 'Smart Solar Charging regio Utrecht', by the Netherlands Enterprise Agency (RVO) in the project 'Slim laden met flexibele nettariëven (FLEET)' and by the European Union's Horizon 2020 research and innovation program under grant agreement No 764786 (project PV-Prosumers4Grid). The authors want to thank Henk Fidder, Robin Berg and Bart van der Ree for their valuable input throughout the research process.

* Corresponding author.

E-mail address: n.b.g.brinkel@uu.nl (N.B.G. Brinkel).

¹ Equal contributions.

Nomenclature*Abbreviations*

aFRR	automatic frequency restoration reserves
BRP	balance responsible party
DA	day-ahead
DSO	distribution system operator
ENTSO-E	European Network of Transmission System Operators
EV	electric vehicle
LV	low-voltage
MV	medium-voltage
OPF	optimal power flow
PV	photovoltaic
ToU	time-of-use
TSO	transmission system operator
V2G	vehicle-to-grid

*EV charging model**Indices and sets*

$k \in \mathcal{K}$	bins in the range of emissions
$s \in \mathcal{S}$	subsets of EV charging transactions
$t \in \mathcal{T}$	timesteps in the assessment period

Parameters

η_{ch}	EV charging efficiency
η_{disch}	EV discharging efficiency
c	electricity price
g	electricity emission factor
Δt	duration of one timestep
$E_{\text{ch,min}}$	minimum accumulated charging energy
$E_{\text{ch,max}}$	maximum accumulated charging energy
$P_{\text{ch,max}}$	maximum charging power
$P_{\text{disch,max}}$	maximum discharging power
P_{PV}	PV generation
P_{res}	residential load
$P_{\text{tr,max}}$	transformer capacity
ϵ	maximum emissions
C_{batt}	battery investment costs
G_{batt}	battery production emissions

Variables

C_{battdeg}	battery degradation costs
C_{el}	electricity costs
C_{grid}	annualized grid reinforcement costs
C_{system}	system costs
G_{battdeg}	battery degradation emissions
G_{el}	electricity emissions
G_{grid}	annualized grid reinforcement emissions
G_{system}	system emissions
P_{ch}	charging power
P_{disch}	discharging power
$P_{\text{grid},t}$	power withdrawn from (+) or injected to (-) the grid
E_{ch}	accumulated charging energy

Battery degradation model

δ	cycle depth of an EV battery system
$\Phi(\delta)$	battery degradation function
b	No. of full equivalent cycles under 100% cycle depth
m	parameter shaping the battery degradation curve
$N_{\text{eol,actual}}$	No. of actual cycles until end of life
$N_{\text{eol,full}}$	No. of full equivalent cycles until end of life

Economic parameters

C_{trans}	costs for upgrading a transformer
C_{cable}	costs for reinforcing one km of electricity cable
G_{trans}	emissions for upgrading a transformer
G_{cable}	emissions for reinforcing one km of electricity cables
l_{cable}	cable length in investigated grid
r	discount rate
L	lifetime of transformer and grid

Appendix

$j \in \mathcal{J}$	set of generation technologies
P_{gen}	generation volume
$P_{\text{gen,CBS}}$	annual generation from CBS
$P_{\text{gen,Transparency}}$	generation in ENTSO-E Transparency Platform
$P_{\text{gen,missing}}$	missing generation in ENTSO-E Trans. Platform
$P_{\text{load,Powerstats}}$	load from ENTSO-E Powerstats
M_{corr}	share of missing generation assigned to a technology

the EVs start charging in the evening hours [1,2]. This causes the EV demand peak to coincide with the evening electricity demand peak of households, inducing grid congestion and power quality problems [3,4]. In addition, uncontrolled charging is not always efficient from a financial and/or CO₂ emission perspective.

In the majority of charging transactions, the EV connection time to the charging station largely exceeds the required time to meet its charging demand [1,5]. This provides the opportunity to optimize the EV charging process by shifting EV charging over time. This process is frequently referred to as smart charging, coordinated charging or controlled charging. Smart charging algorithms have been proposed for a wide range of objectives. The majority of the proposed charging algorithms perform economic optimization of EV charging [6,7]; these algorithms aim to minimize the charging costs of EV owner or aggregators in case of unidirectional charging, or to maximize their economic benefits using vehicle-to-grid (V2G) technology. Other proposed EV smart charging algorithms aim to minimize CO₂ emissions [8], maximize self-consumption of photovoltaic (PV) solar energy [9] or mitigate congestion and power quality problems in LV grids [10,11]. These research activities were followed by actual implementation and testing of smart charging algorithms in real-life environments [12,13].

Numerous business case analyses have demonstrated the economic

attractiveness of smart charging in different electricity markets, with potential financial benefits ranging from 106 €/year to 1008 €/year per EV [14,15]. Despite previous research having illustrated that the specific hourly electricity generation mix is an important moderator of the CO₂ emission impact of EVs [16], emission minimization through smart charging and V2G has only been addressed in a limited number of studies. Some of these studies operationalize this by minimizing the electricity imported from the grid [17,18]. The limitation of this approach is that it fails to recognize that the emission factor of the electricity generation mix also shows large fluctuations over time, depending on the actual dispatch of e.g. renewables, coal- and gas-fired power plants [19]. Others translate emissions to costs and subsequently minimize on these adapted cost functions [20,21]. This eliminates the possibility to do a pure emission-based optimization, and it therefore underestimates the mitigation potential of smart charging and V2G. The limitations of these previous studies can be addressed by constructing emission profiles which can be used as input in the emission optimization process [22,23]. To the best of our knowledge, only Zakariazadeh et al. [24] and Hoehne et al. [8] have applied this approach to smart charging or V2G. However, both studies only consider a short timescale and neglect day-to-day variations in emissions. Battery degradation is also not considered in both studies, while this can have

important implications for the Pareto frontier in battery multi-objective optimization [23]. Furthermore, Hoehne et al. [8] do not determine the trade-off between charging costs and emissions and only consider plug-in hybrid EVs, while Zakariazadeh et al. [24] consider unrealistic synthetic price and emission profiles which overestimate the variability in emissions and prices by a factor of 10 [19,25].

A second gap identified in scientific literature is the limited attention of the potential adverse impact of smart charging and V2G on grid congestion. Increasing grid congestion induced by EV charging can occur when a large set of EVs charge simultaneously at moments with low electricity costs or emissions. Distribution system operators (DSOs) are required to accommodate the needs of all system users and requests for new connections in the LV-grid [26], which could result in increasing need for grid reinforcements in order to accommodate smart charging and V2G. On the one hand, grid reinforcements cause that EVs are less constrained by the grid capacity in minimizing costs and emissions. On the other hand, grid reinforcements result in extra emissions and socialized costs from manufacturing and installing grid assets. This demonstrates the need to determine whether the economic and environmental benefits of smart charging with a higher grid capacity limit outweigh the costs and emissions of grid reinforcements.

This study aims to address the two gaps in literature that were identified above. First, the trade-off between cost and emission minimization of EV charging is determined using multi-objective optimization framework. The second aim is to assess whether it is beneficial from a cost and emission system perspective to reinforce the grid. To do so, the multi-objective framework is used to compare the cost and emission benefits of smart charging with a higher grid capacity limit with the costs and emissions of grid reinforcements. The model uses a method to model the aggregated charging pattern of a large set of EVs at low computational time and considers EV battery degradation, V2G and transformer limits. The model is tested by using an actual case study grid for different EV adoption rates, PV adoption rates, emission profiles and pricing schemes.

This paper is outlined as follows: Section 2 presents the system architecture, discusses a method to model the aggregated charging pattern of a large set of EVs at low computational time and provides the multi-objective optimization problem formulation. Section 3 provides a literature review on battery degradation experiments, determining the empirical relationship between cycle depth and battery degradation. Section 4 introduces the investigated case study and provides an overview of the data inputs. Section 5 presents the multi-objective optimization results, including a sensitivity analysis on the effect of different critical parameters such as EV adoption rate, PV adoption rate and V2G on the outcomes. Lastly, the discussion is presented in Section 6 and conclusions and suggestions for future research are presented in Section 7.

2. Methods

2.1. System architecture

Fig. 1 shows the system architecture of this study. The system boundaries contain a single LV grid, which connects a number of households, PV systems and EV charging stations. Because this research focuses on the cost and emissions from a system perspective, we assume one central operator that controls all loads. In the assessment timeframe, a set of EV charging transactions is conducted at the EV charging stations in the investigated LV grid. The central operator ensures the power flows through the Medium Voltage (MV)/LV transformer remain within the transformer limits, the residential load is satisfied and the charging needs of the EVs are met. EV demand is assumed to be the only shiftable load and furthermore EVs are able to feed electricity into the grid (i.e., V2G). The central operator can control the charging and discharging of the EVs to optimize economic and/or environmental objectives. This study assumes perfect foresight in residential load, PV

generation, time-of-use (ToU) tariffs, emission profiles and EV availability.

2.2. System costs and system emissions

A transformer upgrade and/or cable reinforcements provide EV fleet operators with more freedom in minimizing EV charging costs and/or emissions without being constrained by the grid capacity. However, to evaluate whether transformer or grid reinforcements are desirable from a system perspective, costs and emissions from the production and installation of a transformer and electricity cables should also be taken into account. Costs and emissions associated with battery degradation should also be considered to account for the potential extra battery degradation with V2G compared to unidirectional charging. System costs and emissions are defined in Eqs. (1a) and (1b) as follows:

$$C_{\text{system}} = C_{\text{el}} + C_{\text{battdeg}} + C_{\text{grid}}, \quad (1a)$$

$$G_{\text{system}} = G_{\text{el}} + G_{\text{battdeg}} + G_{\text{grid}}, \quad (1b)$$

where C_{system} and G_{system} are respectively the annual system costs and emissions, C_{el} and G_{el} are the total annual electricity costs and emissions for the whole LV grid, C_{battdeg} and G_{battdeg} are the total annual costs and emissions resulting from EV battery degradation and C_{grid} and G_{grid} are the annualized costs and emissions from grid reinforcements.

Grid reinforcement costs C_{grid} and emissions G_{grid} are annualized by using Eqs. (2a) and (2b):

$$C_{\text{grid}} = \frac{(C_{\text{trans}} + l_{\text{cable}} C_{\text{cable}})r}{(1 - (1 + r)^{-L})} \quad (2a)$$

$$G_{\text{grid}} = \frac{G_{\text{trans}} + l_{\text{cable}} G_{\text{cable}}}{L}, \quad (2b)$$

where C_{trans} and G_{trans} represent the total costs and emissions of producing and replacing a transformer, C_{cable} and G_{cable} represent respectively the costs and emissions for reinforcing one kilometer of cable, l_{cable} represents the total cable length that is reinforced and L represents the assumed lifetime of the grid, assuming that the transformer and the cables have the same lifetime. Grid reinforcement costs are discounted to consider the time value for money; r represents the discount rate.

2.3. Modelling aggregated EV charging patterns

Nearly all EV optimization models optimize the charging behavior of individual EV transactions, since each charging transaction has its unique plug-in time, plug-out time, charging requirement and maximum charging rate (e.g., [27,28]). With high EV penetration, optimization of individual EV transactions could result in a significant computational burden, as each individual EV transaction adds a set of variables to the optimization problem. This computational burden can hinder policymakers and DSOs to perform techno-economic scenario

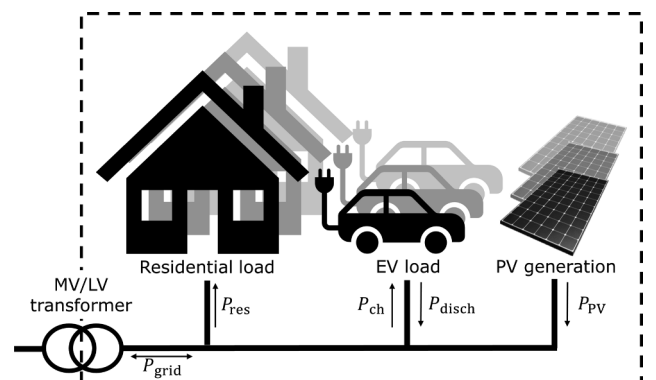


Fig. 1. The proposed system architecture.

studies for a long time horizon and for a large number of case-specific grids, considering a large number of parameters.

A study by Tang et al. [29] has proposed a method to model the aggregated charging behavior of a large pool of EVs in a LV grid at one timestep as a single variable, inducing a considerable reduction in the computational time. The method converts the required charging volume, maximum charging power, plug-in time and plug-out time of individual EV charging transactions into an aggregated maximum charging power ($P_{ch,max,t}$), minimum accumulated charging energy ($E_{ch,min,t}$) and maximum accumulated charging energy ($E_{ch,max,t}$) per timestep for a set of charging transactions, as described in Table 1. This method allows the charging behavior of this set of charging transactions to be modelled as a single community battery with a variable (i.e., time-dependent) battery capacity.

This study proposes two modifications to the methods of Tang et al. [29]. First, this study proposes to model accumulated EV charging behavior as multiple community batteries with a variable battery capacity instead of as a single community battery, since Tang et al.'s methods can underestimate the costs or emissions of EV smart charging: The maximum charging power $P_{ch,max,t}$ is aggregated for multiple EV charging transactions, which allows the model to meet the charging requirement of individual charging transactions by charging with a higher charging power than physically possible for an individual charging transaction. This study proposes to divide the set of EV-transactions into S subsets, where $s \in \mathcal{S} \{1, 2, \dots, S\}$, in a chronological order based on the plug-in time. Subsequently, $P_{ch,max,t,s}$, $P_{disch,max,t,s}$, $E_{ch,max,t,s}$ and $E_{ch,min,t,s}$ are determined for every timestep and for every subset. The number of subsets S can be varied to determine a balance between computational time and accuracy of the model. Second, this study proposes to extend the method of Tang et al. to V2G-systems by introducing a maximum discharging rate ($P_{disch,max,t,s}$) for the aggregated EV charging model. Table 1 discusses the proposed methods for determining $P_{disch,max,t,s}$.

2.4. Multi-objective optimization model formulation

2.4.1. Objective functions and ϵ -constraint

A common approach to address a problem with multiple objectives is to determine the Pareto frontier using the ϵ -constraint method [30]. Each optimization is first solved separately, calculating the two end-points of the Pareto frontier. The cost and emission objective functions are formulated in Eqs. (3a) and (3b):

$$\text{minimize } \sum_{t=1}^T (C_{el,t} + C_{battdeg,t}), \quad (3a)$$

$$\text{minimize } \sum_{t=1}^T (G_{el,t} + G_{battdeg,t}), \quad (3b)$$

where C_{el} represents the electricity costs, $C_{battdeg}$ the battery degradation costs, G_{el} represents the CO₂ emissions related to electricity consumption and $G_{battdeg}$ the CO₂ emissions related to battery degradation. C_{el} and G_{el} can be determined according to Eqs. (4a) and (4b):

$$C_{el,t} = c_t P_{grid,t} \Delta t \quad \forall t, \quad (4a)$$

$$G_{el,t} = g_t P_{grid,t} \Delta t \quad \forall t, \quad (4b)$$

where at timestep t the ToU-tariff is represented by c_t , the emissions related to electricity consumption are represented by g_t and the total amount of electricity withdrawn from (+) or injected to (-) the MV-grid is represented by $P_{grid,t}$.

Additional discharging and charging of an EV impacts the lifetime of the EV battery caused by cyclic ageing [31,32]. Therefore, it is important to include battery degradation into the objective function, to ensure batteries are only discharged and charged if the benefits exceed the costs associated to battery degradation. If δ represents the cycle depth of an EV battery system, then the battery degradation costs $C_{battdeg}$ and degradation emissions $G_{battdeg}$ at timestep t can be calculated using Eqs. (5a) and (5b):

$$C_{battdeg,t} = C_{batt} \sum_{s=1}^S \Phi(\delta_{s,t}) \quad \forall t, \quad (5a)$$

$$G_{battdeg,t} = G_{batt} \sum_{s=1}^S \Phi(\delta_{s,t}) \quad \forall t, \quad (5b)$$

where C_{batt} are the battery investment costs and G_{batt} are the emissions from producing a battery. The dimensionless degradation function $\Phi(\delta_{s,t})$ is discussed in Section 3.

The minimum and maximum of the range in emissions are the outcome of Eq. (3b), and the emissions associated to the optimal solution found in Eq. (3a), respectively. Subsequently, the range in emissions is divided into K equally spaced bins ϵ_k , where $k \in \mathcal{K} \{1, 2, \dots, K\}$. The ϵ -constraint can now be formulated by treating the emission function 3b as a constraint for each bin ϵ_k , as in Eq. (6), and running the problem using the cost objective:

$$\sum_{t=1}^T (G_{el,t} + G_{battdeg,t}) \leq \epsilon_k. \quad (6)$$

This approach allows to obtain the least-cost solution for a certain intended reduction in emissions. Only the cost minimization runs of the multi-objective optimization are subject to this constraint. The objective functions (3a) and (3b) are subject to various other constraints, as discussed in the following sections.

2.4.2. Power balance constraint

The power balance constraint is formulated in Eq. (7):

$$P_{grid,t} = P_{res,t} - P_{PV,t} + \frac{1}{\eta_{ch}} \sum_{s=1}^S P_{ch,s,t} - \eta_{disch} \sum_{s=1}^S P_{disch,s,t} \quad \forall t, \quad (7)$$

where $P_{res,t}$ and $P_{PV,t}$ represent the residential load and PV generation in the investigated LV grid at timestep t . These are assumed to be non-controllable. $P_{ch,s,t}$ and $P_{disch,s,t}$ represent, respectively, the charging and discharging power at the EV battery of EV group s at timestep t and η_{ch} and η_{disch} represent the EV charging and discharging efficiencies.

Table 1

Overview of parameters for optimizing the aggregated charging demand of EV transaction subset s , adapted based on Tang et al. [29].

$E_{ch,max,t,s}$	The maximum accumulated charging energy at timestep t of EV set s is equal to the required charging energy of all EVs of transaction set s that connected to the grid between $t = 0$ and t .
$E_{ch,min,t,s}$	The minimum accumulated charging energy assures that the charging requirement of individual charging transactions is met before unplugging. $E_{ch,min,t,s}$ is equal to accumulated charging volume of all EVs in transaction set s that connected to the grid between $t = 0$ and t in the 'latest charging scenario'. The 'latest charging' scenario assumes that the charging schedule of an EV is delayed to the latest and that an EV charges at maximum charging power in the required number of timesteps to meet its charging demand before unplugging.
$P_{ch,max,t,s}$	The maximum charging power of EV set s at timestep t is equal to the maximum charging power of all EVs of EV transaction set s connected to the grid at timestep t .
$P_{disch,max,t,s}$	The maximum discharging power of EV set s at timestep t is equal to the maximum discharging power of all EVs of EV transaction set s connected to the grid at timestep t , excluding EVs that are charging in the latest charging scenario at timestep t . This avoids the model to discharge at maximum power one timestep before an EV unplugs, resulting in unmet charging demand.

2.4.3. Charging power constraints

The aggregated charging and discharging power of each subset of EVs are constrained by a maximum charging and discharging power, which are determined using the methods presented in Section 2.3:

$$0 \leq P_{ch,t,s} \leq P_{ch,max,t,s} \quad \forall t, s, \quad (8)$$

$$0 \leq P_{disch,t,s} \leq P_{disch,max,t,s} \quad \forall t, s. \quad (9)$$

2.4.4. Accumulated charging energy constraints

To model the charging behavior of a group of EVs as a single community battery, the accumulated charging energy is constrained by a minimum and maximum accumulated charging energy, as discussed in Section 2.3:

$$E_{ch,min,t,s} \leq E_{ch,t,s} \leq E_{ch,max,t,s} \quad \forall t, s, \quad (10)$$

where $E_{ch,t,s}$ is a variable that represents the accumulated charging energy of EV group s at timestep t . $E_{ch,t,s}$ is based on the accumulated charging energy in the previous timestep and the charging and discharging power at timestep t :

$$E_{ch,t,s} = 0 \text{ for } t = 1, \forall s. \quad (11)$$

$$E_{ch,t,s} = E_{ch,t-1,s} + (P_{ch,t,s} - P_{disch,t,s})\delta t \quad \forall t \in \{2 \dots T\}, s. \quad (12)$$

2.4.5. Transformer capacity constraint

To avoid transformer overloading, $P_{grid,t}$ is constrained by the transformer capacity ($P_{tr,max}$) at every timestep t , as formulated in Eq. (13):

$$-P_{tr,max} \leq P_{grid,t} \leq P_{tr,max} \quad \forall t. \quad (13)$$

Since residential load and PV generation are assumed to be non-controllable in this study, only EV charging behavior is altered to meet this constraint.

3. Battery degradation

Wöhler curves, or Stress – Number of cycles curves (S-N curves), are often used to predict material fracture under cycle loading [33]. This relation can also be applied to cyclic battery degradation [34]. Doing this, the relation between number of full equivalent cycles until end of life $N_{eol,full}$ and cycle depth δ takes the following general form:

$$N_{eol,full} = b\delta^m. \quad (14)$$

By default, parameter b reflects the number of cycles under cycle depth of 100% (i.e., $\delta = 1$), whereas battery degradation parameter m determines the specific shape of the curve. To obtain the number of actual cycles $N_{eol,actual}$ until end of life, one needs to correct for the actual cycle depth:

$$N_{eol,actual} = \frac{b\delta^m}{\delta} = b\delta^{m-1}. \quad (15)$$

The degradation per cycle of the battery is the inverse of $N_{eol,actual}$. Considering half cycles instead of full cycles, this can be translated to the dimensionless degradation function $\Phi(\delta_{s,t})$:

$$\Phi(\delta_{s,t}) = \frac{0.5}{b\delta^{m-1}} = \frac{0.5}{N_{eol,actual}}. \quad (16)$$

Note, as this function is non-linear, Eqs. (5a), (5b) and (6) are treated as piecewise linear functions in the optimization model by using four segments.

A literature review was performed to determine appropriate values for the parameters b and m for lithium-ion EV batteries. Fig. 2 shows the results of seven different studies; all studies comply to the general form presented in Eq. (14), with the R^2 for each individual study ranging from 0.92 to 1.00. For every cycle depth that was researched by more than four studies, the average value of $N_{eol,actual}$ was taken. A trendline with the form of Eq. (14)

was fitted using the MATLAB curve fitting toolbox; values of b and m were determined at $4084 (\pm 367; 95\% \text{ confidence})$ and $-0.7514 (\pm 0.0324)$, respectively, with an adjusted R^2 of 0.997. These values are used as battery degradation parameters in this study.

4. Data inputs

4.1. Case study specifications

This research considers an LV grid in a residential area in the Lombok district in Utrecht (the Netherlands) as a case study grid. This part of the distribution grid is used as a living lab in the Smart Solar Charging research project [12] to determine the impact of EV charging and PV generation on LV grids. For this research project, EV charging transaction data is logged from 26 EV charging stations and the PV generation from three PV systems is logged on a 5-min basis.

The investigated grid has a radial outline and is connected to the MV grid through a 400 kVA transformer. The total cable length equals 3.3 km, divided over 19 feeder lines. Most cables in the grid are made out of copper, with cross-sectional areas ranging from 25 to 95 mm², as described in [40]. The total electricity demand in this grid equaled 1251 MWh in 2017.

The transformer capacity in this grid can be upgraded to 630 kVA. This study will compare the system costs and system emissions with and without transformer upgrades.

4.2. EV charging transactions

The analyses in this study are performed for different EV adoption rates, as depicted in Table 2. Future sets of EV charging transactions are generated to reflect high EV adoption rates, using the methods described in [5] and using two years of logged EV charging data from the investigated grid. The different EV adoption rates in Table 2 represent the share of EVs in total number of cars possessed by households connected to the investigated grid, considering the current car possession rate of 0.4 car/household in the Lombok district [41]. Table 2 makes a distinction between local EVs and other EVs (e.g., visiting EVs), using the classification method in [5]. It is assumed that all electric vehicles in the future are battery electric vehicles (BEVs) and that the ratio between local EVs and other EVs is the same as in the logged EV data.

4.3. Grid reinforcement costs and emissions

Table 3 shows general values for the costs and emissions of grid

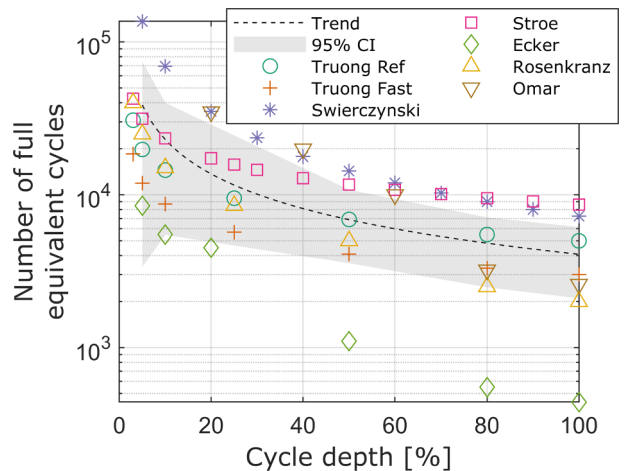


Fig. 2. Cycle depth versus number of full equivalent cycles. Data from [32,35–39]. Trendline is an exponential fit of the averages of the studies; the 95% CI is the confidence interval of the mean for every cycle depth.

Table 2
Details of the sets of EV transactions used.

EV adoption	No. EVs charging per year		No. charging transactions per year	EV charging volume per year
	Local	Other		
25%	34	916	7339	132 MWh
50%	68	1832	14464	257 MWh
75%	102	2749	20778	372 MWh
100%	136	3665	28355	506 MWh

reinforcements used in economic and environmental assessments about grid reinforcements. In this study, we consider both scenarios with only transformer upgrades and scenarios in which 25%, 50%, 75% and 100% of the cables in the grid are reinforced. Table 4 presents the annualized reinforcement costs and emissions for each considered scenario, which are based on Eqs. (2a) and (2b).

4.4. Emission profiles and other data input

Table 5 provides an overview of the data inputs used in this study. The emission profiles form an important input for this study. Two different profiles are composed for the Netherlands in 2018: an average emission profile and a marginal emission profile. These are constructed according to the methods presented in [16,19]; more details can be found in Appendix A. Average emission profiles are constructed by taking the weighted average emission factors of all electricity generating technologies in a certain time frame (15 min in this study). This makes them especially suitable for CO₂ accounting purposes. Marginal emission profiles take the emission factor of one specific power plant, namely the one that is the price-setting unit in a certain time frame (typically one hour). An increase or decrease of demand leads to altered electricity generation of this power plant, which makes these profiles very suitable to determine the emission impact of charging optimization [46].

The assessment time horizon equals one year. To limit the computational burden of the simulation, the EV charging optimization is split into individual months, which are subsequently combined to obtain the annual total electricity and battery costs. The simulation of each month also considers the EV charging transactions starting in the five days before the start of the month to assure that a representative number of EVs is charging at the beginning of the month. In addition, five days after the last day of the month are considered in each monthly optimization to allow EVs to finish their charging transaction. Battery degradation was only considered in simulations with V2G functions, as V2G can increase battery degradation compared to unidirectional EV charging. The number of EV subsets S equalled 50 for 25% EV adoption, 150 for 50% EV adoption, 200 for 75% EV adoption and 250 for 100% EV adoption, based on Section 5.3. Simulation was performed in Python [47] with the Gurobi [48] solver, using a laptop equipped with an Intel i7-5600U processor and a 16 GB RAM.

5. Results

5.1. Multi-objective optimization results

The Pareto frontier showing the trade-off between cost minimization and emission minimization for EV charging is presented in Fig. 3. This figure shows the trade-off for both marginal and average emissions and identifies the impact of a transformer upgrade from 400 kVA to 630 kVA on system costs and emissions.

5.1.1. Unidirectional charging

Fig. 3 indicates that cost minimization of unidirectional EV charging with a 400 kVA transformer results in a reduction of charging costs of 22.7% compared to uncontrolled charging. Emission minimization of EV charging with a 400 kVA transformer can reduce charging emissions

Table 3
Overview of parameter values used in this study for determining annualized grid reinforcement costs and emissions.

C_{trans} (630 kVA)	€15,000 [42]
C_{cable}	120,000 €/km [42]
G_{trans} (630 kVA)	136.3 tCO ₂ eq ^a [43]
G_{cable}	12.5 tCO ₂ eq/km ^b [44]
r	3% [42]
L	40 years [42]
l_{cable}	3.3 km

^a Jorge et al. [43] determined the life-cycle emissions for a 315 kVA transformer. This has been scaled to a 630 kVA transformer by using a scale factor of 0.8 [45]. Emissions from transformer losses were not considered, assuming that a transformer upgrade of 400 to 630 kVA does not result in additional transformer losses.

^b This study assumes that underground copper cables are replaced with aluminum cables. The emissions from the production and installation of an aluminum cable are combined with the end-of-life emission benefits of copper cables.

Table 4
Overview of annualized grid reinforcement costs and emissions with different shares of cable reinforcements.

% of cables reinforced	Annualized costs	Annualized emissions
0%	649 €/year	3.41 t CO ₂ eq/year
25%	4955 €/year	3.67 t CO ₂ eq/year
50%	9262 €/year	3.93 t CO ₂ eq/year
75%	13568 €/year	4.19 t CO ₂ eq/year
100%	17225 €/year	4.44 t CO ₂ eq/year

by 8.0% when considering average emission profiles and by 23.6% when considering marginal emission profiles. Even with 100% emission minimization of EV charging, costs are reduced by 7.8% compared to uncontrolled charging when considering average emission profiles and by 13.2% when using marginal emission profiles.

Marginal emission profiles show a larger spread in emissions compared to average emission profiles (standard deviations in 2018 of 0.190 kg CO₂eq/kWh and 0.045 kg CO₂eq/kWh respectively, see also Figs. A1 and A2 in Appendix A), as a change in marginal power plant (e.g., from a coal- to a gas-fired power plant) has a direct substantial impact on the marginal emission factor. The impact of a different marginal power plant on the average emission factor is limited, since a large share of the total emissions are determined by relatively constant baseload generation.

Fig. 3 indicates that the increase in costs when shifting from cost minimization to emission minimization is higher when using average emissions profiles than when using marginal emission profiles. An explanation can be found in the input data: the lowest values of marginal emission factors coincide with lower prices than the lowest values of average emission factors. The lowest marginal emission factors are found in hours in which the most efficient gas-fired power plant is marginal; this implies a relatively low residual electricity demand, and thus relatively low prices.

Overall, the CO₂-abatement costs² when shifting from cost-based optimization to emission-based optimization range from 2.8 to 22.6 €/tCO₂eq with increasing levels of emission abatement when considering marginal emission profiles with a 400 kVA transformer. The CO₂-abatement costs range from 21.8 to 310.6 €/tCO₂eq when considering average emission profiles.

² CO₂-abatement costs are calculated by dividing the increase in system costs when shifting from cost minimization towards a partly emission-based charging optimization by the decrease in system emissions when making this shift.

Table 5
Overview of data inputs in this study.

PV-generation profiles	Normalized 15-min data (kW/kWp) from three logged PV systems in the Lombok district in Utrecht, the Netherlands.
Residential load profiles	Standardized household load profiles from NEDU [49] and the total annual electricity consumption of all grid connections in the investigated grid in 2017.
Price data	Day-ahead market prices in the Netherlands in 2018 in most runs. automatic Frequency Restoration Reserve (aFRR) imbalance prices in the Netherlands in 2018 in Section 5.2.2
Emission profiles	Average emission profiles are determined using the method in [19] and 15-min generation data in 2018 from the Netherlands from [25]. Marginal emission profiles are determined using the methods in [16] and Dutch day-ahead market prices in 2018. Specific assumptions can be found in Appendix A.
η_{ch}, η_{disch}	$\sqrt{0.87}$ [50]
Δt	15-min
Battery degradation parameters	Parameters presented in Section 3.
Battery investment costs	130 €/kWh [51]
Battery production emissions	104 kg CO ₂ eq/kWh [52]

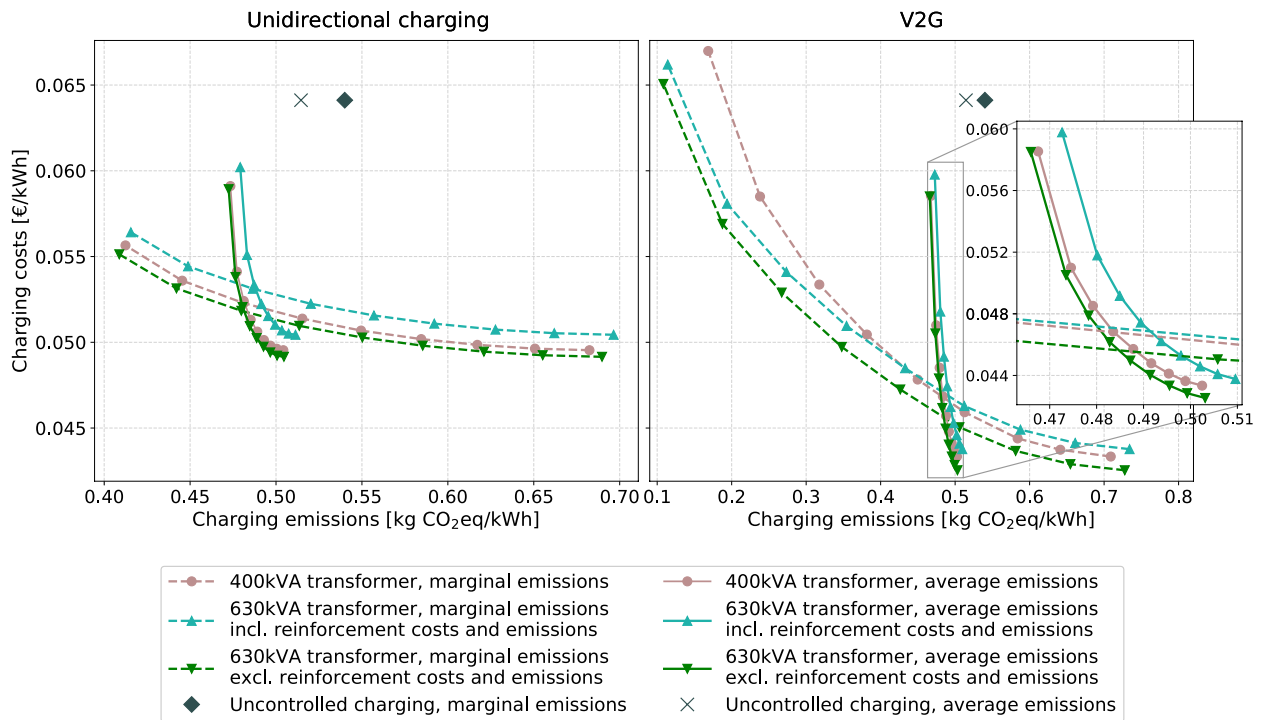


Fig. 3. Pareto frontier for multi-objective optimization of costs and CO₂-emissions of EV charging, considering average and marginal emission profiles and considering unidirectional charging (left) and V2G (right). Pareto frontiers are presented for an EV adoption rate of 100% and an installed PV capacity of 400 kWp. Battery degradation costs and emissions are considered for all Pareto frontiers. For V2G, the costs and emissions are presented per net charged kWh (i.e., charging volume minus discharging volume).

5.1.2. V2G

V2G functions allow for a larger reduction in charging costs and emissions, as EVs can inject electricity to the grid at moments with high costs or emissions. Fig. 3 shows that the cost reduction potential of V2G compared to uncontrolled charging equals 32.4%, whereas the emission reduction potential equals 8.7% when using average emission profiles and 67.3% when using marginal emission profiles. This emission reduction with V2G is most profound for marginal emission profiles due to its high volatility in emissions. This high volatility causes that the emission benefits of discharging exceed the extra battery degradation emissions, resulting in high discharging volumes when minimizing emissions with marginal emission profiles. This also explains why the increase in EV charging costs with V2G is higher with marginal emission profiles when shifting from cost-based optimization to emission-based optimization. EV discharging volumes are higher when optimizing emissions using marginal emission profiles. This causes EVs to

inject electricity to the grid at moments with high emissions, corresponding to low electricity prices, thus increasing the net charging costs of EV charging. The CO₂-abatement costs when shifting from cost-based optimization to emission-based optimization range from 5.9 to 43.8 €/tCO₂eq for marginal emissions and from 82.7 to 434.8 €/tCO₂eq for average emissions when considering V2G functions with a 400 kVA transformer.

5.1.3. Impact of transformer upgrade

Comparing the Pareto frontiers corresponding to 400 kVA and 630 kVA transformers in Fig. 3 provides insight on the effect of a transformer upgrade on system costs and emissions. The results indicate that EV charging costs and emissions are lower with a 630 kVA transformer from the perspective of the central operator (i.e., when neglecting transformer upgrading costs and emissions), since this Pareto frontier is located below the 400 kVA Pareto frontier in all scenarios. A

transformer upgrade causes that EVs are less constrained in their charging behavior by the transformer capacity, providing more freedom to EVs in minimizing their charging costs or emissions. However, Fig. 3 shows that with unidirectional charging, a transformer upgrade is never beneficial from a system perspective in terms of both costs and emissions when also considering the costs and emissions for producing and installing a transformer.

A transformer upgrade has a more pronounced impact on system costs and emissions with V2G, since EVs are not only less frequently constrained by the transformer capacity during charging, but also less constrained during discharging. This allows EVs to inject more electricity to the grid at moments with beneficial prices and/or emissions. With V2G, the Pareto frontiers corresponding to the transformer capacities of 400 and 630 kVA (including transformer upgrading costs and emissions) intersect at EV charging emissions of 0.45 kg CO₂eq/kWh. This indicates that grid reinforcements are attractive from a system perspective in the investigated case study when constraining the EV charging emissions to 0.45 kg CO₂eq/kWh or lower when EVs optimize their charging schedule using V2G.

5.2. Sensitivity analysis on system impact of grid reinforcements

To provide better insights under what circumstances grid reinforcements are beneficial from a system perspective, this section elaborates on how the system impact of grid reinforcements changes with different values for critical parameters, including the EV adoption rate, installed PV capacity, selected pricing scheme and level of grid reinforcement. These sensitivity analyses focus on the impact on system costs, since most DSOs still base decisions for grid reinforcements on financial grounds.

5.2.1. Impact of EV adoption rate and installed PV capacity

Fig. 4 presents a breakdown of the change in system costs with a transformer upgrade from 400 kVA to 630 kVA for different EV adoption rates and different installed PV capacities for both unidirectional charging and V2G. Fig. 4 indicates that in all cases with both unidirectional EV charging and V2G, the annualized investments outweigh the reduction in EV charging costs due to a transformer upgrade, resulting in an increase in system costs. An increase in total system costs implies that from a system perspective, under the assumptions in this study, it is not economically attractive to reinforce the grid to mitigate congestion problems induced by EVs.

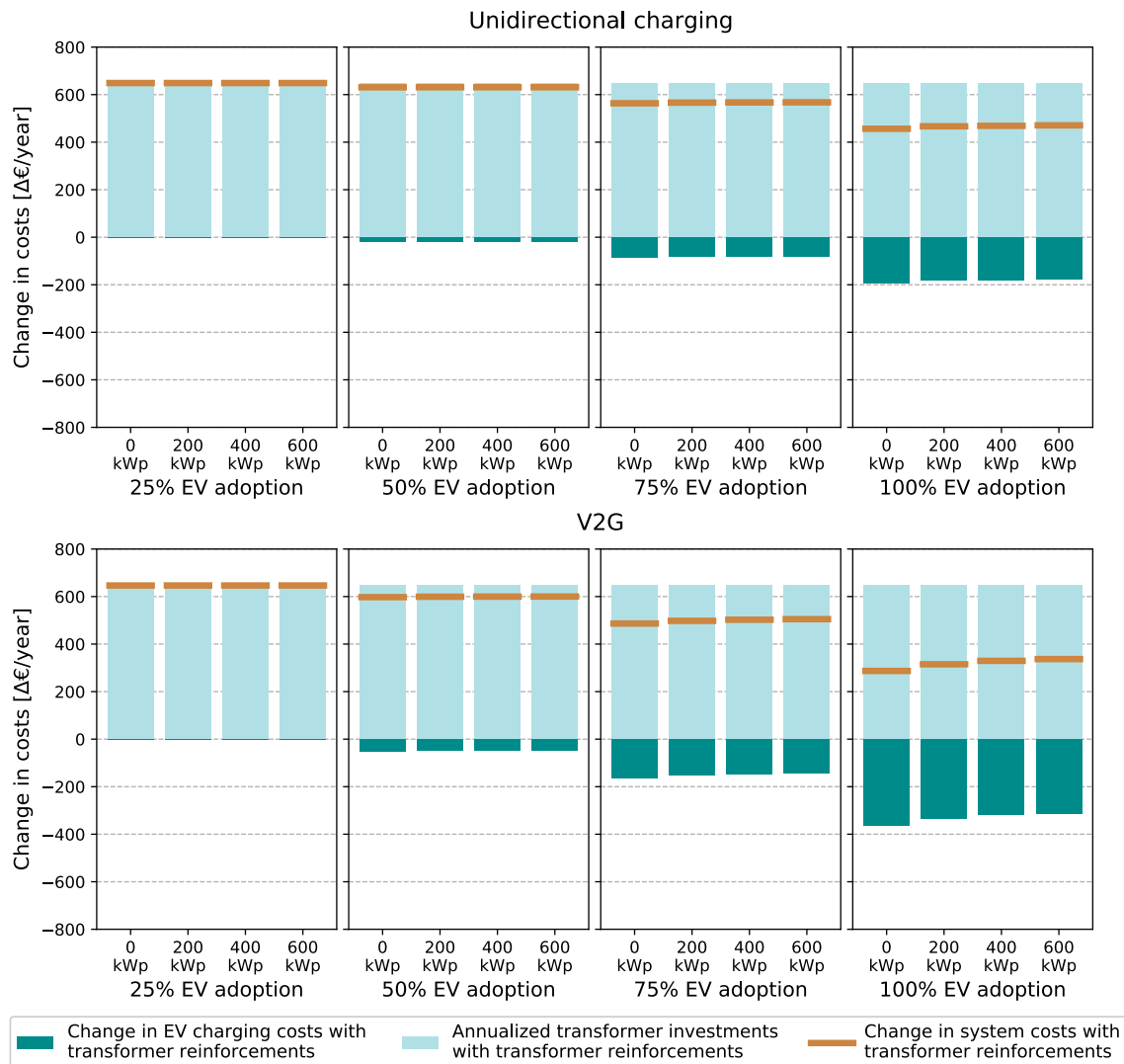


Fig. 4. Annualized transformer investments, change in EV charging costs and change in system costs with a transformer upgrade of 400 kVA to 630 kVA in the investigated grid for different EV adoption rates and installed PV capacities with unidirectional charging (top) and bidirectional charging (bottom). No cable reinforcements are considered in this figure.

A transformer upgrade leads to a larger decrease in EV charging costs with higher EV adoption rates. As a high EV load can cause transformer overloading, the number of times that EVs are constrained by the transformer capacity in charging at moments with low prices increases with the number of EVs connected to the grid. Subsequently, a transformer upgrade leads to a larger reduction in EV charging costs with higher EV adoption rates.

The decrease in EV charging costs with a transformer upgrade is lower with a higher installed PV capacity in the grid. PV generation causes that less power withdrawal from the MV grid is required to fulfil the electricity demand of EVs. As a consequence, EVs can meet a larger share of their charging demand at moments with low electricity prices without causing transformer overloading, thus a transformer upgrade has a less pronounced effect on the EV charging costs.

5.2.2. Impact of selected pricing scheme

With increasing integration of renewables into the electricity system, electricity prices could become more volatile. In addition, it is unlikely that all EVs will be subject to the same price-incentives as inputs in the optimization of their charging process, since EVs are optimized in the context of different (sub-) markets via the central operator. To determine how these developments could affect the impact of grid reinforcements on system costs, additional simulations were performed in which different shares of the EV fleet used the more volatile Dutch automatic Frequency Restoration Reserves (aFRR) prices in optimizing their charging schedule.

Fig. 5 indicates that the decrease in EV charging costs with grid reinforcements outweighs the grid reinforcement investments when a large number of EVs bases its charging schedule on aFRR prices, using the scenario of 100% EV adoption with a 200 kWp installed PV capacity in the considered LV grid. This highlights the major impact of the volatility of the selected pricing scheme on the outcome of the analysis. The effect is less pronounced with a low share of EVs using aFRR prices to optimize their charging behavior compared to a situation where all EVs use day-ahead market prices in their optimization process, as the most beneficial prices for EV charging do not occur at the same moments for both pricing schemes. Consequentially, EV demand peaks are better distributed over time, resulting in fewer moments in which the charging demand is constrained by the transformer capacity.

5.2.3. Impact of level of grid reinforcement

Fig. 6 presents the change in system costs with different levels of cable reinforcement for a situation where 100% of the EVs are optimized based on the aFRR prices. This is the situation with the largest decrease in EV charging costs with grid reinforcements. The annualized grid investments rise sharply when grid reinforcements are required next to a transformer upgrade, since cable reinforcements require costly excavations. Even with high price volatility, grid reinforcements are not beneficial from a system perspective if a large share of the cables in the grid need to be reinforced.

5.3. Accuracy of EV community battery modelling method

Fig. 7 compares the computational time and objective outcome of conventional methods for optimizing EV charging behavior (i.e., creating variables for every individual charging transactions) with the computational time and objective outcome when using the methods proposed in Section 2.3. The results indicate that when the aggregated EV charging demand is optimized using one subset of EV charging transactions, as proposed by Tang et al. [29], the annual EV charging emissions are underestimated by 7.0% with a 100% EV adoption rate when considering marginal emission profiles. The underestimation in objective outcome equals 1.8% when optimizing using average emission profiles, 6.6% when optimizing using day-ahead prices and 12.5% when optimizing using aFRR prices. Increasing the number of subsets rapidly reduces this charging cost or emission estimation error, until

this error is completely eliminated. The computational running time increases with a larger number of subsets, allowing users of the proposed method to make a trade-off between computational time and estimation error in results. Fig. 7 indicates that aggregated EV charging demand can be optimized using a cost estimation error of 1% at a relative computational time of below 20% compared to conventional EV charging optimization methods. With lower EV adoption, a lower number of subsets is required to eliminate the inaccuracy in optimizing EV charging costs.

6. Discussion

This study presented Pareto frontiers to get insight in the trade-off between cost-based optimization and emission-based optimization of EV charging in an LV-grid under different transformer capacity limits. A model was developed to be able to optimize EV charging for a large group of EVs at lower computational cost compared to conventional EV optimization models, without losing accuracy in results. The results show that grid reinforcements to mitigate grid congestion caused by EV charging are in most situations not beneficial from both a cost and emission perspective; the additional costs and emissions in case of reinforcement outweigh the potential additional EV charging optimization benefits that can be obtained as a result of the higher transformer capacity. These results are robust for various future scenarios regarding the penetration of PV and EVs, but not with much more volatile electricity prices. A second major finding was that even with the current transformer limitations, the costs and emissions related to EV charging can be decreased substantially. For example, emission-based charging optimization can reduce charging marginal emissions by 23.6% compared to uncontrolled EV charging, while also reducing the costs by 13.2%. With V2G, marginal emission savings of up to 67.3% are possible, while charging costs can be reduced by 32.4%.

These findings have important practical implications. For example, a transition from internal combustion engine vehicles to EVs can have a larger impact on emissions than often assumed - also on the short term. This could help countries in attaining their climate goals. Many studies consider the average generation mix to estimate the impact of this transition, whereas this study shows that EVs are adept to be charged with electricity that is less CO₂ intensive than the average of a country's generation mix.

Further, it was shown that a high penetration of EVs is possible under the current transformer limit for the investigated grid, and moreover, the current transformer limit provides ample possibilities for smart charging and V2G. In order for such a system to function, various

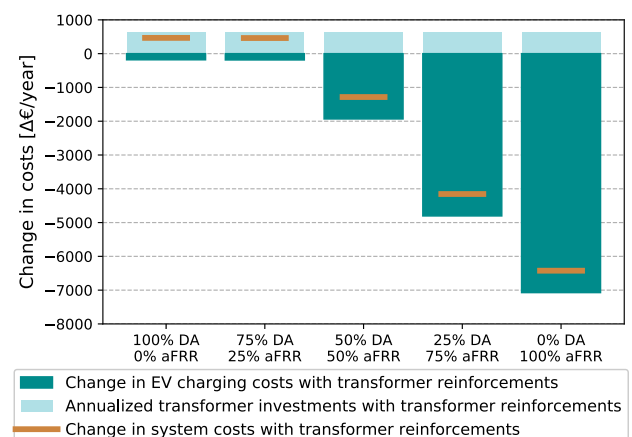


Fig. 5. Annualized transformer investments, change in electricity costs and change in electricity costs with a transformer upgrade of 400 kVA to 630 kVA in the investigated grid for different shares of cars charging using aFRR and day-ahead (DA) prices in optimizing their charging process. Results are presented for an EV adoption rate of 100% and an installed PV capacity of 200 kWp.

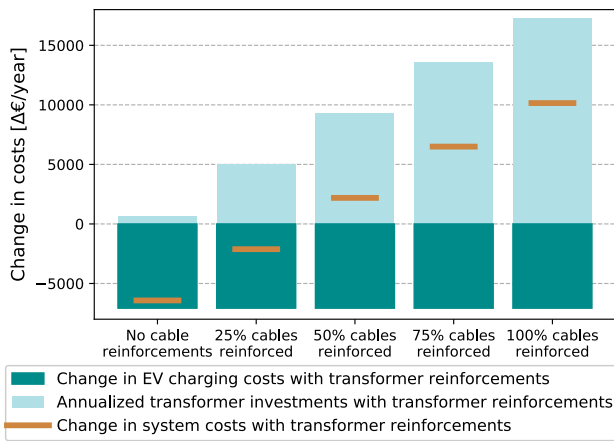


Fig. 6. Annualized grid investments, change in electricity costs and change in electricity costs with a transformer upgrade of 400 kVA to 630 kVA in the investigated grid for different grid reinforcement scenarios. Results are presented for an EV adoption rate of 100% and an installed PV capacity of 200 kWp. All EVs in this scenario used aFRR prices to optimize their charging demand.

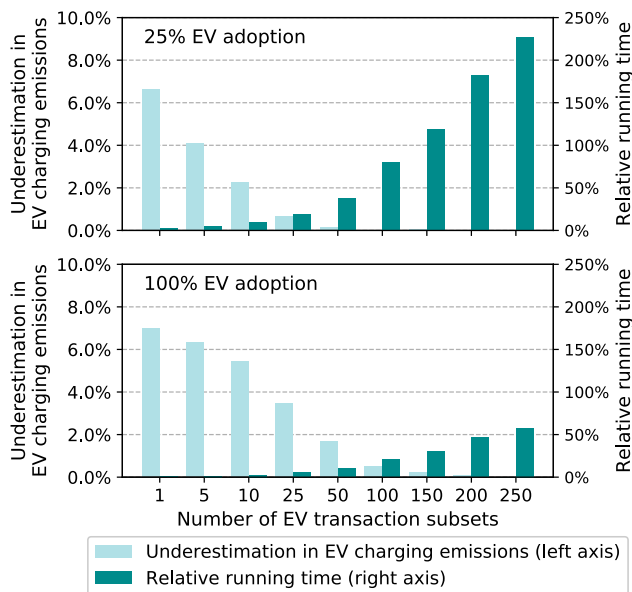


Fig. 7. Underestimation in model outcome and relative computational running time of the aggregated EV charging model proposed in Section 2.3 using different numbers of EV charging transaction subsets. The model outcome and computational time of a conventional EV charging model formulation is taken as the reference. Installed PV capacity equals 200 kWp. EVs used marginal emission profiles to optimize their charging demand.

options exist. One option is that the DSO enforces central operators to stay within the overall capacity limits, with the DSO as single buyer, and the charging fleet operators providing ancillary services (e.g., see [53]). This option will require investments in communication infrastructure.

Currently DSOs are legally obliged to accommodate the needs of all system users [26], which could mean that charging fleet operators should be financially compensated when they are constrained by the grid capacity. It should be reconsidered whether this system can be maintained in the future in grids with high EV adoption. An important recommendation is to think of a new framework which allows for a socially fair distribution of costs and benefits.

Two main categories of uncertainty should be considered when interpreting the results: uncertainty in input data and uncertainty in forecasting accuracy. One of the main sources of uncertainty in the input data are the used emission profiles. To determine the marginal emission profile, this study assumed marginal emissions are equal to the emissions of the plant with marginal costs closest to day-ahead market price. As discussed in [19], it is not always possible to determine the actual marginal power plant. More accurate marginal emission profiles can only be constructed if each balance responsible party (BRP) publishes the CO₂ intensity of their scheduled generation based on the unit commitment of their power plants. Given the large emission reduction potential of EV charging when optimizing EV charging using marginal emission factors, this study recommends countries or regions to publish live marginal emission factors to facilitate adoption of emission-based smart charging. These emission factors should be published in such a way that market-sensitive information of electricity generating companies is not revealed.

In addition, there is uncertainty regarding the future robustness of the price input data. The trade-off between cost minimization and emission minimization EV charging is heavily dependent on the CO₂-price. With higher CO₂-prices, gas-fired power plants can become cheaper than coal-fired power plants, resulting in a merit order with alternating coal- and gas-fired power plants. A further increasing CO₂-price could make the trade-off between costs and emissions less severe, as electricity can be shifted to times with low emissions for lower or low additional costs. A last important notion in this context is the penetration of renewables. Higher penetration of renewables leads to a higher variation in emission profiles [16] and potentially leads to higher price volatility, which would increase the width of the Pareto frontiers.

This study assumed a perfect forecasting accuracy in PV generation, residential load, electricity prices, electricity generation emission factors and EV availability when scheduling the charging behavior of EVs. Although multiple studies have developed forecasting methods which could be applied to LV grids, forecast errors could be relatively large, especially since this study looks at a relatively small aggregation level (a single LV grid). Due to these forecast errors, grid congestion problems cannot be fully eliminated, causing that real-time correction of the charging schedule of EVs is required to mitigate risks on grid congestion problems. In addition, due to these imperfect forecasts, EVs might be charged more conservatively in practice to avoid grid congestion or unmet EV charging demand requirements. Thus, the actual potential of EVs to minimize costs or emissions may be lower than the theoretical potential identified in this study.

Although this study has concluded that grid reinforcements are not attractive in terms of cost and emissions from a system perspective when the focus is on congestion problems caused by deep penetration of EV charging in LV grids, our sensitivity analysis also suggested that this could be different with more volatile prices. Furthermore, it should be noted that the decision whether to reinforce the grid is based on multiple factors. Grid reinforcements are not only a solution to grid congestion problems, but could also be necessary to mitigate power quality problems [54]. Next to the large-scale integration of EVs, these problems could also be caused by i.a. greater penetration of variable renewable energy sources in the LV grid or electrification of space heating and cooking in buildings.

7. Conclusion and future research

This research addressed the question whether grid reinforcements are attractive from a cost or emission perspective in the context of a deep penetration of EVs. It was shown that the costs and emissions of grid reinforcements outweigh the benefits in costs and emissions in EV charging optimization resulting from increased grid capacity. However, substantial reductions in EV charging costs and emissions can be

achieved under the current transformer capacity.

Future research could study to what extent it is possible to avoid grid congestion problems when using forecasts of the expected grid load when scheduling EV charging with a transformer capacity constraint. This research should compare the grid congestion levels with different forecasting methods that are used with EV charging scheduling and should also evaluate different methods to mitigate grid congestion induced by forecast errors. Also, future research could look further into the economic and environmental attractiveness of grid reinforcements by using more-realistic EV charging schedules, which consider different electricity markets and uncertainty in EV departure times. Furthermore, future research could address when LV grid reinforcements are required from a technical perspective when considering congestion and power quality problems caused by greater penetration of variable renewable electricity generation in the LV grid, as well as the electrification of end-uses in buildings.

Appendix A. Assumptions emission profiles

The 15-min average emission profiles and marginal emission profiles can be found in Figs. A1 and A2. The same methods were used as in [19,16], respectively. However, some assumptions and modifications were made to adapt the profiles to the year 2018.

CRediT authorship contribution statement

N.B.G. Brinkel: Conceptualization, Methodology, Writing - original draft, Writing - review & editing, Visualization. **W.L. Schram:** Conceptualization, Methodology, Writing - original draft, Writing - review & editing, Visualization. **T.A. AlSkaif:** Writing - review & editing, Supervision. **I. Lampropoulos:** Writing - review & editing, Supervision. **W.G.J.H.M. Sark:** Writing - review & editing, Supervision, Funding acquisition.

Declaration of Competing Interest

The authors declare that they have no known competing financial interests or personal relationships that could have appeared to influence the work reported in this paper.

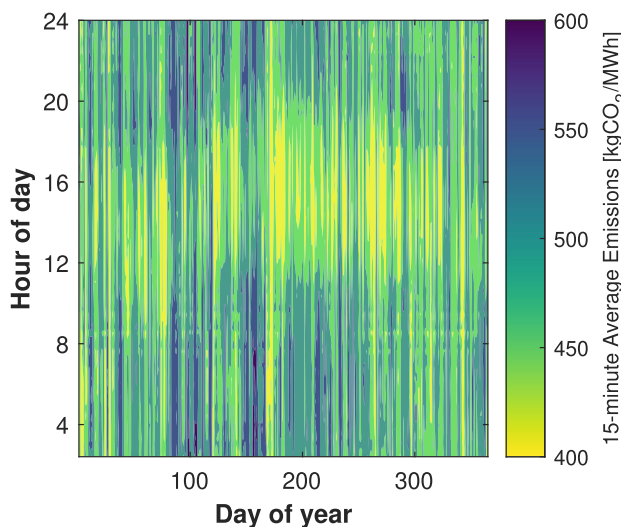


Fig. A1. 15-min average emission profile for the Netherlands in 2018.

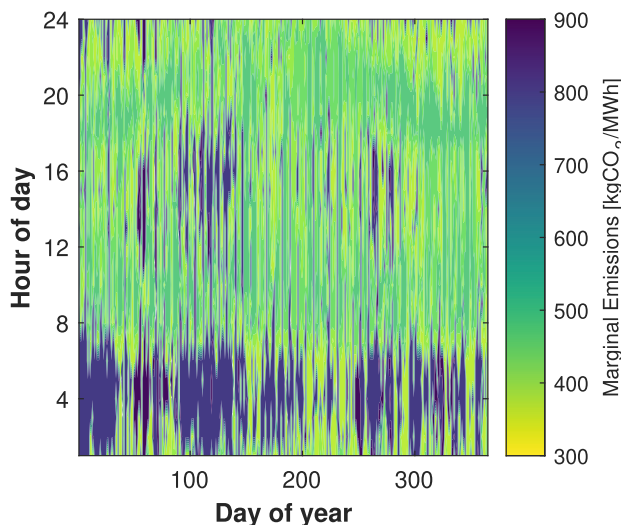


Fig. A2. Marginal emission profile for the Netherlands in 2018.

A.1. 15-min average emission profiles

Because of missing data in [25], some data modifications had to be performed. When generation data of a specific technology for one hour was missing, data was filled using the forward fill method, i.e., data of the previous hour was used. When data of more than one hour was missing, the data of the previous day was used.

ENTSO-E Transparency Platform [25] provides generation values for biomass generation and solar generation. However, these values are low compared to official Dutch statistics [55]. Therefore, data was scaled to be in line with these statistics.

Subsequently, the remaining missing power generation in time step t was determined using the following equation:

$$P_{\text{gen,missing},t} = P_{\text{load,Powerstats},t} + P_{\text{netexport},t} - \sum_j P_{\text{gen,Transparency},j,t} \quad (17)$$

i.e., the sum of the net export and the total Dutch electricity load taken per timestep from ENTSO-E Powerstats [56] was subtracted by the total known generation power of technology j , with J being the total number of technologies provided by ENTSO-E Transparency Platform. For gas-fired and coal-fired electricity generation, ENTSO-E Transparency Platform provides for 2018 a part of the data and no data, respectively. For these technologies, it was determined which fraction M_{corr} of the $P_{\text{gen,missing},t}$ could be attributed the generation of technology j :

$$M_{\text{corr},j} = \frac{\sum_t (P_{\text{gen,Transparency},j,t}) - P_{\text{gen,CBS},j}}{\sum_t P_{\text{gen,missing},t}} \quad (18)$$

Now, the $P_{\text{gen},j,t}$ of coal- and gas-fired power plants could be determined using:

$$P_{\text{gen},j,t} = P_{\text{gen,Transparency},j,t} + M_{\text{corr},j} P_{\text{gen,missing},t} \quad (19)$$

A.2. Marginal emission profiles

Three modifications were carried out compared to [16]. First, data for the fuel prices was taken from [57]. Second, the least efficient gas-fired power plant was assumed to be the Merwede-11 plant. Hence, the Velsen-24 plant, which is fired by blast-furnace gas, was excluded from the analysis. Third, a factor representing the upstream emissions was included, taken from [58].

References

- [1] Sadeghianpourhamami N, Refa N, Strobbe M, Devellder C. Quantitative analysis of electric vehicle flexibility: A data-driven approach. *Int J Electr Power Energy Syst* 2018. <https://doi.org/10.1016/j.ijepes.2017.09.007>. ISSN: 01420615.
- [2] Kim JD. Insights into residential EV charging behavior using energy meter data. *Energy Policy* 2019. <https://doi.org/10.1016/j.enpol.2019.02.049>. ISSN: 03014215.
- [3] Quiros-Tortos J, Ochoa L, Butler T. How electric vehicles and the grid work together. *IEEE Power Energy Mag*. 2018(October 2018).
- [4] Papadopoulos P, Skarvelis-Kazakos S, Grau I, Cipcigan LM, Jenkins N. Electric vehicles' impact on British distribution networks. *IET Electrical Syst Transport* 2012;2(3):91–102. <https://doi.org/10.1049/iet-est.2011.0023>. ISSN: 20429738.
- [5] Gerritsma MK, AlSkaif TA, Fidder HA, van Sark WG. Flexibility of electric vehicle demand: analysis of measured charging data and simulation for the future. *World Electric Vehicle J* 2019;10(1):14. <https://doi.org/10.3390/wevj10010014>. ISSN: 2032-6653.
- [6] Garcia-Villalobos J, Zamora I, San Martin JI, Asensio FJ, Aperribay V. Plug-in electric vehicles in electric distribution networks: A review of smart charging approaches, 2014. doi: 10.1016/j.rser.2014.07.040.
- [7] Daina N, Sivakumar A, Polak JW. Modelling electric vehicles use: a survey on the methods, 2017. doi: 10.1016/j.rser.2016.10.305.
- [8] Hoehne CG, Chester MV. Optimizing plug-in electric vehicle and vehicle-to-grid charge scheduling to minimize carbon emissions. *Energy* 2016. <https://doi.org/10.1016/j.energy.2016.39.057>. ISSN: 03605442.
- [9] van der Kam M, van Sark W. Smart charging of electric vehicles with photovoltaic power and vehicle-to-grid technology in a microgrid; a case study. *Appl Energy* 2015. <https://doi.org/10.1016/j.apenergy.2015.04.092>. ISSN: 03062619.
- [10] Hu J, Saleem A, You S, Nordstrom L, Lind M, Ostergaard J. A multi-agent system for distribution grid congestion management with electric vehicles. *Eng Appl Artif Intell* 2015. <https://doi.org/10.1016/j.engappai.2014.10.317>. ISSN: 09521976.
- [11] Cheng L, Chang Y, Huang R. Mitigating voltage problem in distribution system with distributed solar generation using electric vehicles. *IEEE Trans Sustainable Energy* 2015. <https://doi.org/10.1109/TSTE.2015.2444390>. ISSN: 19493029.
- [12] Smart Solar Charging, About Smart Solar Charging. [Online]. Available: <https://smartsolarcharging.eu/en/about-smart-solar-charging/>.
- [13] TenneT, Europe's first blockchain project to stabilize the power grid launches: TenneT and sonnen expect results in 2018 - TenneT, 2017. [Online]. Available: <https://www.tennet.eu/news/detail/europes-first-blockchain-project-to-stabilize-the-power-grid-launches-tennet-and-sonnen-expect-res/>.
- [14] Schuller A, Dietz B, Flath CM, Weinhardt C. Charging strategies for battery electric vehicles: Economic benchmark and V2G potential. *IEEE Trans Power, Syst* 2014;29(5):2014–222. <https://doi.org/10.1109/TPWRS.2014.2301024>. ISSN: 08858950.
- [15] Gough R, Dickerson C, Rowley P, Walsh C. Vehicle-to-grid feasibility: A techno-economic analysis of EV-based energy storage. *Appl Energy* 2017. <https://doi.org/10.1016/j.apenergy.2017.01.102>. ISSN: 03062619.
- [16] Schram W, Louwen A, Lampropoulos I, van Sark W. Comparison of the greenhouse gas emission reduction potential of energy communities. *Energies* 2019;12(4440):1–23. <https://doi.org/10.3390/en12234440>.
- [17] Das R, Wang Y, Putrus G, Kotter R, Marzband M, Herteleer B, Warmerdam J. Multi-objective techno-economic-environmental optimisation of electric vehicle for energy services. *Appl Energy*. 2020;257(September 2019):113–965, doi: 10.1016/j.apenergy.2019.113965. [Online]. Available: <https://doi.org/10.1016/j.apenergy.2019.113965>. ISSN: 03062619.
- [18] Anand MP, Mohan V, Ongsakul W, Suresh MP. Optimal day ahead scheduling of distributed EVs in a smart distribution network. In: *Proceedings of the 2015 IEEE Innovative Smart Grid Technologies - Asia, ISGTASIA 2015*, 2015. doi: 10.1109/ISGT-Asia.2015.7387133.
- [19] Schram W, Lampropoulos I, AlSkaif T, Sark WV. On the Use of Average versus Marginal Emission Factors. In: *8th International Conference on Smart Cities and Green ICT Systems (SMART-GREENS 2019)*, Heraklion: SciTePress, 2019, p. 187–93, ISBN: 000000217804. [Online]. Available: <http://www.insticc.org/Primoris/Resources/PaperPdf.ashx?idPaper=77657>.
- [20] Lu X, Zhou K, Yang S, Liu H. Multi-objective optimal load dispatch of microgrid with stochastic access of electric vehicles. *J Clean Produc* 2018;195:187–99. <https://doi.org/10.1016/j.jclepro.2018.05.190> ISSN: 09596526. [Online]. Available: <https://doi.org/10.1016/j.jclepro.2018.05.190>.
- [21] Huang Q, Jia QS, Xia L, Guan X. Event-based optimization for stochastic matching EV charging load with uncertain renewable energy. In: *Proceedings of the World Congress on Intelligent Control and Automation (WCICA)*, vol. 2015-March, 2015, no. March, p. 794–799, doi: 10.1109/WCICA.2014.7052817.
- [22] Lokeshgupta B, Sivasubramani S. Multi-objective dynamic economic and emission dispatch with demand side management. *Int J Electr Power Energy Syst*. 2018;97(November 2017):334–43, doi: 10.1016/j.ijepes.2017.11.020. [Online]. Available: <https://doi.org/10.1016/j.ijepes.2017.11.020>. ISSN: 01420615.
- [23] Schram WL, AlSkaif T, Lampropoulos I, Henein S, Sark Wv. On the trade-off between environmental and economic objectives in community energy storage operational optimization. *IEEE Trans Sustainable Energy* 2020. <https://doi.org/10.1109/TSTE.2020.2969292>.
- [24] Zakariazadeh A, Jadid S, Siano P. Multi-objective scheduling of electric vehicles in smart distribution system. *Energy Convers Manage* 2014;79:43–53. <https://doi.org/10.1016/j.enconman.2013.11.042> [Online]. Available: <https://doi.org/10.1016/j.enconman.2013.11.042>. ISSN: 01968904.
- [25] ENTSO-E, ENTSO-E Transparency Platform, 2019. [Online]. Available: <https://transparency.entsoe.eu/> (visited on 02/19/2020).

- [26] Dutch Ministry of Economic Affairs and Climate, Elektriciteitswet, Artikel 24, 1998.
- [27] Zhang K, Xu L, Ouyang M, Wang H, Lu L, Li J, Li Z. Optimal decentralized valley-filling charging strategy for electric vehicles. *Energy Convers Manage* 2014. <https://doi.org/10.1016/j.enconman.2013.11.011>. ISSN: 01968904.
- [28] Janjic A, Velimirovic L, Stankovic M, Petrusic A. Commercial electric vehicle fleet scheduling for secondary frequency control. *Electric Power Syst Res* 2017. <https://doi.org/10.1016/j.epr.2017.02.019>. ISSN: 03787796.
- [29] Tang Y, Zhong J, Bollen M. Aggregated optimal charging and vehicle-to-grid control for electric vehicles under large electric vehicle population. *IET Generat, Transmiss Distrib* 2016;10(8):2012–8. <https://doi.org/10.1049/iet-gtd.2015.0133>. ISSN: 1751-8687.
- [30] Deb K. *Multi-objective optimization using evolutionary algorithms*. 16th ed. John Wiley & Sons; 2001.
- [31] Truong CN, Naumann M, Karl RC, Müller M, Jossen A, Hesse HC. Economics of residential photovoltaic battery systems in Germany: The case of tesla's powerwall. *Batteries*, 2016;2(2), doi: 10.3390/batteries2020014. ISSN: 23130105.
- [32] Rosenkranz CA, Kohler U, Liska JL. Modern battery systems for plug-in hybrid electric vehicles. In: 23rd International Battery and Fuel Cell Electric Vehicle Symposium and Exposition (EVS 23); 2007.
- [33] Miner MA. Cumulative damage in fatigue. *J Appl Mech* 1945;12(3):A159–64.
- [34] Magnor D, Gerschler JB, Ecker M, Merk P, Sauer DU. Concept of a battery aging model for lithium-ion batteries considering the lifetime dependency on the operation strategy. In: 24th European Photovoltaic Solar Energy Conference, Hamburg, 2009, p. 3128–34, ISBN: 3-936338-25-6. doi: 10.4229/24thEUPVSEC2009-4BO.11.3.
- [35] Truong C, Naumann M, Karl R, Müller M, Jossen A, Hesse H. Economics of residential photovoltaic battery systems in Germany: The Case of Tesla's Powerwall. *Batteries* 2016;2(2):14. <https://doi.org/10.3390/batteries2020014> [Online]. Available: <http://www.mdpi.com/2313-0105/2/2/14>. ISSN: 2313-0105.
- [36] Swierczynski M, Stroe DI, Stan AI, Teodorescu R, Kaer SK. Lifetime estimation of the Nanophosphate LiFePO4 battery chemistry used in fully electric vehicles. *IEEE Trans Ind Appl* 2015;51(4):3453–61. <https://doi.org/10.1109/TIA.2015.2405500>. ISSN: 00939994.
- [37] Stroe DI, Knap V, Swierczynski M, Stroe AI, Teodorescu R. Operation of a grid-connected lithium-ion battery energy storage system for primary frequency regulation: A battery lifetime perspective. *IEEE Trans Ind Appl* 2017;53(1):430–8. <https://doi.org/10.1109/TIA.2016.2616319>. ISSN: 00939994.
- [38] Ecker M, Nieto N, Kabitz S, Schmalstieg J, Blanke H, Wamecke A, et al. Calendar and cycle life study of Li(NiMnCo)O2-based 18650 lithium-ion batteries. *J Power Sources* 2014;248:839–51. <https://doi.org/10.1016/j.jpowsour.2013.09.143> [Online]. Available: <https://doi.org/10.1016/j.jpowsour.2013.09.143>. ISSN: 03787753.
- [39] Omar N, Monem MA, Firouz Y, Salminen J, Smekens J, Hegazy O, et al. Lithium iron phosphate based battery - Assessment of the aging parameters and development of cycle life model. *Appl Energy* 2014;113:1575–85. <https://doi.org/10.1016/j.apenergy.2013.09.003> [Online]. Available: <https://doi.org/10.1016/j.apenergy.2013.09.003>. ISSN: 03062619.
- [40] Brinkel N, Gerritsma M, AlSkaif T, Lampropoulos I, van Vo-orden A, Fidler H, et al. Impact of rapid PV fluctuations on power quality in the low-voltage grid and mitigation strategies using electric vehicles. *Int J Electr Power Energy Syst* 2020;118. <https://doi.org/10.1016/j.ijepes.2019.105741>.
- [41] CBS Statline, Kerncijfers buurten en wijken 2017, 2017. [Online]. Available: <https://www.cbs.nl/nl-nl/maatwerk/2017/31/kerncijfers-wijken-en-buurten-2017>.
- [42] Tractebel, Optimale integratie van elektrisch vervoer, PV, warmtepompen in bestaand energiesysteem - Meeting 29/05/2018, Tech. Rep., 2018.
- [43] Jorge RS, Hawkins TR, Hertwich EG. Life cycle assessment of electricity transmission and distribution-part 2: Transformers and substation equipment. *Int J Life Cycle Assess* 2012;17(2):184–91. <https://doi.org/10.1007/s11367-011-0336-0>. ISSN: 09483349.
- [44] Turconi R, Simonsen CG, Byriel IP, Astrup T. Life cycle assessment of the Danish electricity distribution network. *Int J Life Cycle Assess* 2014;19(1):100–8. <https://doi.org/10.1007/s11367-013-0632-y>. ISSN: 09483349.
- [45] Blok K, Nieuwlaar E. *Introduction to energy analysis*. Routledge; 2016.
- [46] Bigazzi A. Comparison of marginal and average emission factors for passenger transportation modes. *Appl Energy*. 2019;242(November 2018):1460–66, doi: 10.1016/j.apenergy.2019.03.172. [Online]. Available: <https://doi.org/10.1016/j.apenergy.2019.03.172>. ISSN: 03062619.
- [47] Python Software Foundation, Python Language Reference. [Online]. Available: <https://docs.python.org/3/reference/>.
- [48] Gurobi, Gurobi Optimizer. [Online]. Available: <https://www.gurobi.com/>.
- [49] NEDU, Profielen elektriciteit 2017 (Electricity profiles 2017), 2017.
- [50] Whitehead A, Smith CL, Grace JM. Vehicle-to-grid fleet demonstration prototype assessment, Lincoln Laboratory, Massachusetts Institute of Technology, Tech. Rep. June, 2018.
- [51] IRENA, Electricity storage and renewables: Costs and markets to 2030, Tech. Rep. October, 2017, p. 132. [Online]. Available: <http://irena.org/publications/2017/Oct/Electricity-storage-and-renewables-costs-and-markets>.
- [52] Hao H, Mu Z, Jiang S, Liu Z, Zhao F. GHG Emissions from the production of lithium-ion batteries for electric vehicles in China. *Sustainability*. 2017;9(4), doi: 10.3390/SU9040504. ISSN: 20711050.
- [53] Lampropoulos I, AlSkaif T, Blom J, Van Sark W. A framework for the provision of flexibility services at the transmission and distribution levels through aggregator companies. *Sustainable Energy, Grids Networks* 2019;17:100187. <https://doi.org/10.1016/j.segan.2018.100187>.
- [54] Bayer B, Matschoss P, Thomas H, Marian A. The German experience with integrating photovoltaic systems into the low-voltage grids. *Renew Energy* 2018;119:129–41. <https://doi.org/10.1016/j.renene.2017.11.045>. ISSN: 18790682.
- [55] Statistics Netherlands (CBS), Electricity and heat; production and input by energy commodity, 2019. [Online]. Available: <https://opendata.cbs.nl/statline/%7B%5C#%7D/CBS/en/dataset/80030eng/table?ts=1582128073786>.
- [56] ENTSO-E, Power Stats, 2019. [Online]. Available: <https://www.entsoe.eu/data/power-stats/> (visited on 10/01/2019).
- [57] Energate, Marktdaten, 2020. [Online]. Available: <https://www.energate-messenger.de/markt/>.
- [58] Louwen A. Comparison of the life cycle greenhouse gas emissions of shale gas, conventional fuels and renewable alternatives from a Dutch perspective. *EBN, Tech. Rep.*, 2011, p. 76. [Online]. Available: <http://www.ebn.nl>.